

Image Capture: Modelling and Calibration of Sensor Responses and their Synthesis from Multispectral Images

Poorvi L. Vora, Joyce E. Farrell, Jerome D. Tietz,
David H. Brainard
Computer Peripherals Laboratory
HPL-98-187
November, 1998

digital cameras,
hyperspectral,
multispectral, sensors,
simulation, modelling,
calibration

This paper describes (a) models for digital cameras, (b) the calibration of the spectral response of a camera and (c) the performance of an image capture simulator. The general model underlying the simulator assumes that the image capture device contains multiple classes of sensors with different spectral sensitivities and that each sensor responds in a known way to light intensity over most of its operating range. The input to the simulator is a set of narrow-band images of the scene taken with a custom-designed hyperspectral camera system [1]. The parameters for the simulator are: the number of sensor classes; the sensor spectral sensitivities; the noise statistics and number of quantization levels for each sensor class; the spatial arrangement of the sensors; and the exposure duration. The output of the simulator is the raw image data that would have been acquired by the simulated image capture device.

To test the simulator, we acquired images of the same scene both with the hyperspectral camera [1] and with a calibrated Kodak DCS-200 digital color camera. We used the simulator to predict the DCS-200 output from the hyperspectral data. The agreement between simulated and acquired images validated the image capture response model, the spectral calibrations, and our simulator implementation. We believe the simulator will provide a useful tool for understanding the effect of varying the design parameters of an image capture device.

Internal Accession Date Only

© Copyright Hewlett-Packard Company 1998

1 Introduction

In this paper we describe, using the Kodak DCS-200 and the DCS-420 as examples, how one can model the sensor response of a camera, calibrate the camera, and then use the model and camera calibration to simulate the camera's response to a scene.

The light sensors in many modern image capture devices (e.g. digital scanners and digital cameras) are based on Charge-Coupled Device (CCD) or Active Pixel Sensor (APS) technology. These devices are usually designed so as to have linear intensity-response functions over most of their operating range [3]. The overall camera system may not exhibit the underlying device linearity, however. For example, there may be a non-linear mapping between the raw sensor output and the digital responses actually available from the camera. Such a non-linearity might be designed into a camera system if the quantization precision of the sensor itself is larger than that of the camera. This is the situation with the Kodak DCS-420. It employs a 12-bit internal data representation for measurements that are linear with respect to light intensity, but its standard control software provides only 8-bits of precision and 8-bit output that is non-linear with respect to light intensity. In this paper we describe methods for testing the camera linearity assumption, as well as a method for determining a static-nonlinearity such as the one used on the Kodak DCS-420.

Color cameras require multiple classes of sensors with different spectral sensitivities. By placing color filters in series with either CCD or APS sensors, usually on a pixel-by-pixel basis, such multiple classes can be created. When the color filters are placed in a mosaic pattern, one color per pixel, the cameras are referred to as color filter array (CFA) cameras. In this paper we also describe methods for estimating the spectral sensitivity of each class of sensor in a color acquisition device.

Evaluation of digital camera design parameters has received considerable attention in the recent literature [4]. These evaluations are based on theoretical models of image statistics and simple image quality metrics. A useful complement to the theoretical approach is to evaluate the performance of different camera designs for actual scenes. A difficulty with this approach is that it is not always feasible. This paper describes a method for constructing, testing and evaluating the performance of an image capture device simulator. A reliable simulator provides a means for evaluating

the performance of a complete image capture device design prior to manufacture.

The simulator we describe is based on several simplifying assumptions about the image capture device. These are (a) that the optical system is linear and shift invariant, (b) that the response of the sensors to light at varying intensities and wavelengths is known, and (c) that the sensor noise is additive. The input to the simulator is a hyperspectral image of the scene, which provides the full spectral power distribution of the incident light at every image location. These images are acquired with a custom-built hyperspectral camera system [1]. Given the hyperspectral image, the simulator computes the response of the image capture device using the response models developed in this paper.

This paper is organised as follows. Section 2 describes the work on camera modelling and section 3 describes the work on camera spectral calibration. In section 4 we describe the simulator and present experimental results verifying its accuracy. Section 5 presents conclusions and future directions.

2 Camera models

To test the linearity of the camera response, we measured the intensity-response functions of the Kodak DCS-200 and the Kodak DCS-420 cameras. The DCS-200 contains an 8-bit CCD array while the DCS-420 contains a 12-bit CCD array. For both cameras, images were obtained with a Macintosh host computer using 8-bit drivers provided by Kodak. The camera apertures were kept fixed (at f5.6 for the DCS-200 and at f4 for the DCS-420) for all experiments described in this paper.

Our basic procedure was to take pictures of a non-selective reference surface (PhotoResearch RS-2 reflectance standard) when it was illuminated by light of different intensities and different wavelengths. We illuminated the surface with light from a tungsten source passed through a grating monochrometer (Bausch & Lomb, 1350 grooves/mm) and varied the intensity by placing neutral density filters in the light path. We used a spectrophotometer (PhotoResearch PR-650) to measure directly the spectrum of the light reflected to the camera. Using this set-up, we measured camera

intensity-response functions at several exposure durations for both the DCS-200 and DCS-420 cameras.

For each intensity-response series, we assigned an intensity measure of unity to the light reaching the camera when no neutral density filters were in the light path. The intensity of other test lights in the series was defined relative to the intensity of this light. The relative intensity was determined by finding the scale factor that brought the maximum-intensity spectrum into agreement with the spectrum of the test light.

Both the DCS-200 and DCS-420 have a resolution of 1524×1012 and the RGB sensors for each camera are arranged in a Bayer mosaic pattern [8]. To obtain sensor data from the camera images we subsampled the camera output using this Bayer pattern. To estimate the mean value of the (dark) additive noise, we acquired images with the lens cap on the camera.

2.1 Linear response model

Assuming linearity, the output of a sensor array at grid position (m,n) maybe be approximated as:

$$\mathbf{r}(m, n) \approx e \sum_{k=1}^N \mathbf{s}(m, n, k) \mathbf{c}(m, n, k) \Delta_\lambda \delta^2 + noise \quad (1)$$

where e is the exposure setting, the argument k represents variation with wavelength, $\mathbf{c}(m, n, k)$ is the spectral sensitivity of the sensor at position (m,n) , $\mathbf{s}(m, n, k)$ is the intensity distribution of light incident on the camera at position (m,n) , Δ_λ is the wavelength sampling for the intensity and spectral response functions, δ is the spatial sampling rate (i.e. the distance between contiguous sensors, assumed to be uniform and identical in both horizontal and vertical directions), and *noise* represents the sensor measurement noise. Correct calibration allows us to drop the constant $\Delta_\lambda \delta^2$ in the above sum. In the formulation of equation (1) we neglect optical blur of the camera. This is justified for the moment because we consider only images of the Macbeth ColorChecker Chart (MCC), a low spatial frequency target, where optical blurring is not a critical factor. We also assume that the spectral response of a

single sensor is constant over each pixel and that the wavelength sampling used is fine enough to accurately represent the spectral response.

We conducted extensive experiments on the Kodak DCS-200 to check whether its performance is well-described by the linear response model [6]. We measured three intensity-response series, one each at wavelengths of 450, 530, and 600 nm. For each image, we averaged the R, G, B values over a region of 3000 (60×50) pixels in the center field of the camera. For each wavelength, the exposure duration was chosen so that the light energy was roughly within the dynamic range of the camera. The exposure duration was fixed for all measurements corresponding to one wavelength.

A typical result is shown in Figure 1. The x-axis shows the intensity of the incident light (calculated as described above) and the y-axis shows the camera output value (with the expected value of the noise subtracted). The crosses represent actual data points. The straight lines are fit to the data and constrained to pass through the origin. In fitting the data, we excluded saturated points and points with very low intensities. The good agreement between the data and the fit lines indicate that the DCS-200 has a linear intensity-response function over most of its operating range.

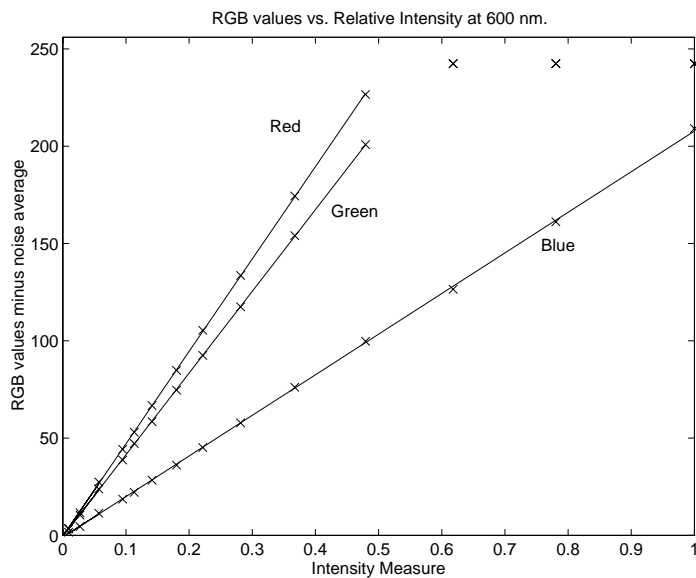


Figure 1: Typical intensity response, DCS-200

We note that the performance of a second digital camera (the Kodak DCS-420) is not

well-described by the linear model, at least when it is operated with the standardly-supplied 8-bit acquisition software [6]. We describe the calibration of the static non-linearity of the Kodak DCS-420 in the next section.

2.2 Static non-linearity model

As shown below, the behavior of the Kodak DCS-420 can be described by a *static non-linearity model*. For this model, the camera response for a pixel of the i^{th} sensor type pixel is given by

$$\mathbf{r}(m, n) \approx \mathcal{F}\left(e \sum_{k=1}^N \mathbf{s}(m, n, k) \mathbf{c}(m, n, k) \Delta_\lambda \delta^2 + \text{noise}\right) \quad (2)$$

where \mathcal{F} is a monotonically increasing non-linear function.

As an initial test of the DCS-420 linearity, we roughly calculated the average green sensor (G) value at the center of the image field for a series of images taken under 525 nm illumination. The relationship between intensity and response was clearly non-linear. A probable cause for this non-linearity is the 12-to-8-bit reduction in the image acquisition software. We performed additional measurements at various wavelengths and exposure durations. We extracted the average R, G, and B sensor readings in the center 64×64 image region. A typical result is plotted in Figure 2 - these measurements were taken under 600 nm illumination and at a 2 sec. exposure setting. In this figure, the expected value of the dark noise has not been subtracted from the camera output. All the results show a similar non-linearity.

2.3 Camera response to variation in exposure

To test for linearity with exposure duration in the Kodak DCS-200, we took pictures of the non-selective reference surface under fixed illumination at different exposure durations. We did this with narrow band illumination at 470, 530, 570 and 660 nm. Figure 3 shows typical results. As with Figure 1, the crosses represent actual data points with the expected value of the noise subtracted and the lines are fits

constrained to pass through the origin. A slight variation from linearity may be due to the fact that the shutter exposure time is not controlled accurately.

As the intensity-response function of the DCS-420 is not linear, it would be surprising if its output were linear with exposure duration. We roughly calculated the average green sensor (G) value at the center of the image field for images of the non-selective reference surface taken at various exposure durations for 525 nm illumination. Figure 4 shows the results with average noise subtracted (x's) overlaid on intensity-response data (replotted as o's). The x-axis represents exposure duration relative to one second and intensity relative to unity. The two readings corresponding to one second and unit intensity are replications of the same illumination condition, so that no scaling of the data were required. The close agreement between the two curves suggests that the same non-linearity mediates both.

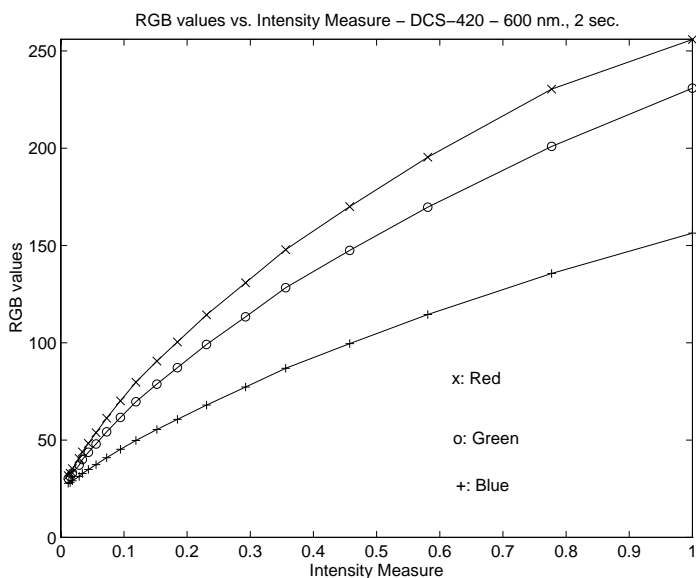


Figure 2: Typical intensity response, DCS-420

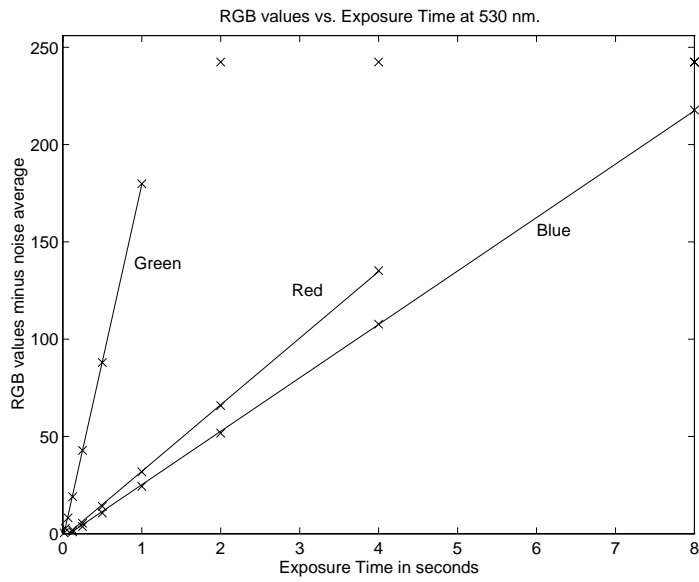


Figure 3: Response vs. exposure duration, DCS-200

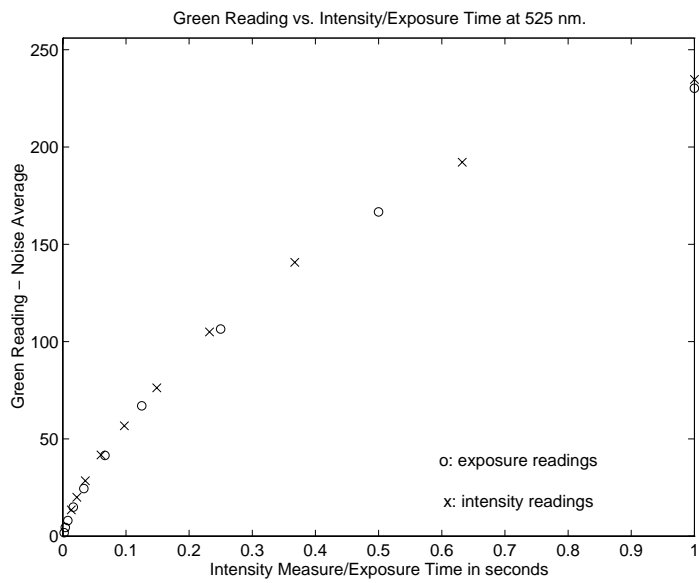


Figure 4: DCS-420: Non-linearity with exposure setting

2.4 Response model summary

2.4.1 Kodak DCS-200

Our data indicate that the linear response model describes the output of the Kodak DCS-200, at least over the output range 20-240 out of a total range of 0-255 camera units. To obtain the parameters describing a single line for all the data, we fit a *calibration line* to the data for the blue sensor readings of Figure 1, DCS-200 readings for incident illumination at 600 nm and 2 second exposure setting *without subtracting out the average dark noise value*. The range of numerical values for the data is 24.98 to 222.71. The fractional values arise because camera raw data readings are averaged over an area to obtain these values. The calibration line is the solid line of Figure 5. Measured camera values on a scale of 0-255 are plotted on the x-axis, while linearized fractional output on a scale of 0-1 is plotted on the y-axis.

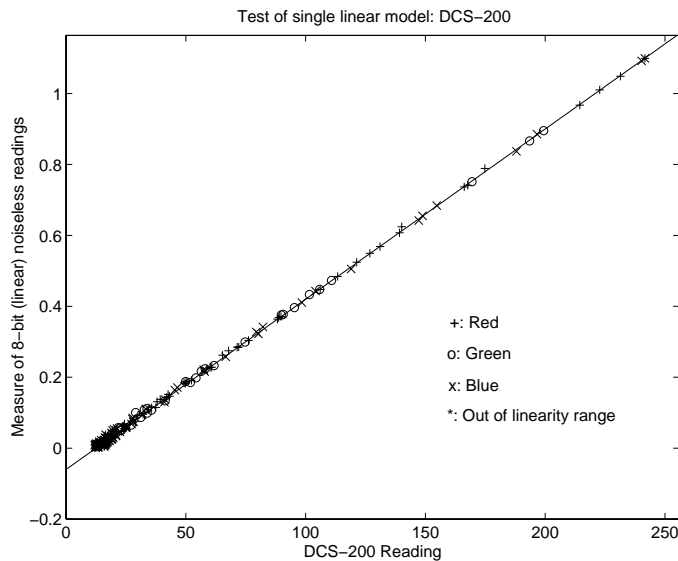


Figure 5: Linearity Map for DCS-200;

To verify that the calibration line derived from one intensity response function describes all the data, we can use this line to normalize all of our data and examine it on a single plot. For each measured intensity response function, the intensity measure we used is arbitrary, since we varied both the exposure and wavelength across

the different measurements. We can use the calibration line to normalize the data, however. For each data set, we found the highest camera output value in the linear range (below 240) and found its position on the calibration line. We then scaled all the intensity values of that data set by a single normalization scale factor such that the highest camera output value in the linear range would correspond to the intensity factor obtained by looking at the calibration line. This procedure allows us to compare all of our data to the calibration line, Figure 5. The highest camera output value for each data set lies on the line because of the way the normalization is performed. Data points with values below 240 and above 20 all lie close to the line. Data points with values below 20 or above 240 are plotted with asterisks (*) or lie outside the region shown in the plot.

2.4.2 Kodak DCS-420

The Kodak DCS-420 is not linear. To examine whether the static non-linearity response model described its performance, we asked how well a single function \mathcal{F} can describe its output across the conditions we measured. We used the intensity-response series measured for the red sensor at 600 nm for a 2 sec exposure (Figure 2) as a reference. This series covered most of the dynamic range of the camera. By interpolating and extrapolating the reference, we obtain a *calibration curve* for the DCS-420 that maps between sensor values (0 to 256) to intensities that lie between 0 and 1. This intensity measure is in arbitrary units but may be calibrated to physical units. (We used the MATLAB [9] function 'griddata', which implements an inverse distance method, to do the interpolation and extrapolation.) The result is tabulated in Table 1 and graphed as the line in Figure 6. It represents the value of $\mathcal{F}^{-1}(r) - n$ (or $e \int_{\lambda_i}^{\lambda_h} s(\lambda)i(\lambda)d\lambda$) of equation (2).

Table 1: Static Nonlinearity, DCS-420

8-bit Input	Linearized Output								
0	0	52	0.0519	103	0.1930	154	0.3820	205	0.6280
1	0	53	0.0541	104	0.1960	155	0.3870	206	0.6330
2	0	54	0.0563	105	0.2000	156	0.3910	207	0.6380
3	0	55	0.0585	106	0.2030	157	0.3960	208	0.6440
4	0	56	0.0607	107	0.2060	158	0.4000	209	0.6490
5	0	57	0.0629	108	0.2090	159	0.4050	210	0.6540
6	0	58	0.0651	109	0.2130	160	0.4100	211	0.6590
7	0	59	0.0674	110	0.2160	161	0.4140	212	0.6650
8	0	60	0.0697	111	0.2190	162	0.4190	213	0.6700
9	0	61	0.0720	112	0.2230	163	0.4240	214	0.6750
10	0	62	0.0743	113	0.2260	164	0.4290	215	0.6810
11	0	63	0.0767	114	0.2300	165	0.4330	216	0.6870
12	0	64	0.0792	115	0.2330	166	0.4380	217	0.6920
13	0	65	0.0816	116	0.2370	167	0.4430	218	0.6980
14	0	66	0.0841	117	0.2400	168	0.4480	219	0.7040
15	0	67	0.0865	118	0.2440	169	0.4520	220	0.7100
16	0	68	0.0890	119	0.2480	170	0.4570	221	0.7160
17	0	69	0.0915	120	0.2510	171	0.4620	222	0.7220
18	0	70	0.0940	121	0.2550	172	0.4670	223	0.7280
19	0.0001	71	0.0965	122	0.2590	173	0.4720	224	0.7340
20	0.0005	72	0.0990	123	0.2630	174	0.4760	225	0.7400
21	0.0009	73	0.1010	124	0.2670	175	0.4810	226	0.7470
22	0.0014	74	0.1040	125	0.2700	176	0.4860	227	0.7540
23	0.0019	75	0.1060	126	0.2740	177	0.4910	228	0.7600
24	0.0025	76	0.1090	127	0.2780	178	0.4960	229	0.7670
25	0.0032	77	0.1120	128	0.2820	179	0.5000	230	0.7750
26	0.0041	78	0.1140	129	0.2860	180	0.5050	231	0.7820
27	0.0050	79	0.1170	130	0.2890	181	0.5100	232	0.7900
28	0.0060	80	0.1200	131	0.2930	182	0.5150	233	0.7970
29	0.0072	81	0.1220	132	0.2970	183	0.5200	234	0.8050
30	0.0086	82	0.1250	133	0.3000	184	0.5250	235	0.8130
31	0.0101	83	0.1280	134	0.3040	185	0.5300	236	0.8220
32	0.0122	84	0.1310	135	0.3080	186	0.5350	237	0.8300
33	0.0148	85	0.1340	136	0.3110	187	0.5400	238	0.8380
34	0.0164	86	0.1370	137	0.3150	188	0.5440	239	0.8470
35	0.0177	87	0.1410	138	0.3180	189	0.5490	240	0.8560
36	0.0195	88	0.1440	139	0.3220	190	0.5540	241	0.8640
37	0.0216	89	0.1470	140	0.3260	191	0.5590	242	0.8730
38	0.0238	90	0.1500	141	0.3290	192	0.5640	243	0.8820
39	0.0260	91	0.1530	142	0.3330	193	0.5690	244	0.8910
40	0.0281	92	0.1570	143	0.3370	194	0.5740	245	0.9000
41	0.0299	93	0.1600	144	0.3410	195	0.5790	246	0.9090
42	0.0314	94	0.1630	145	0.3450	196	0.5840	247	0.9180
43	0.0327	95	0.1670	146	0.3480	197	0.5890	248	0.9270
44	0.0343	96	0.1700	147	0.3520	198	0.5940	249	0.9360
45	0.0363	97	0.1730	148	0.3560	199	0.5990	250	0.9450
46	0.0384	98	0.1770	149	0.3610	200	0.6040	251	0.9550
47	0.0407	99	0.1800	150	0.3650	201	0.6090	252	0.9640
48	0.0430	100	0.1830	151	0.3690	202	0.6130	253	0.9730
49	0.0453	101	0.1870	152	0.3730	203	0.6180	254	0.9830
50	0.0475	102	0.1900	153	0.3780	204	0.6230	255	0.9920
51	0.0497								

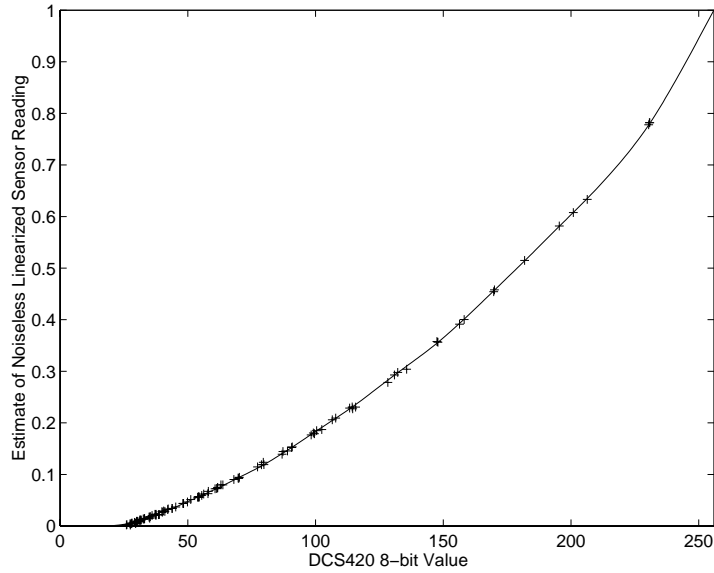


Figure 6: Calibration Curve for DCS-420.

We tested the accuracy of the calibration curve by asking how well it described the rest of our data. Each set of acquired data points has a different intensity scale. A value of unit intensity corresponds to the maximum intensity for the shutter speed used for that test. To check if the other acquired data points lie on the calibration curve, the intensity values need to be transformed to a single scale. We calculated the scale factor for the conversion for each data set by using the highest measured output value (which corresponds to a unit intensity for that series), finding its position on the calibration curve, and using the fractional intensity value thus obtained as the scale factor. The data points from all of our intensity-response series as well as the exposure data are plotted in Figure 6 along with the calibration curve. The data all lie along the curve.

2.5 Variation from Model

The data points vary slightly from the linear model for the DCS-200 and from the calibration curve for the DCS-420. In this section, we quantify the variation.

To estimate the slight variation from linearity of the DCS-200, we calculated the differences between values predicted by the straight line in the linearity plot of Figure 5 and actual values, for measured values above 20 and below 240. These differences are plotted in Figure 7. This calculation assigns zero difference to the maximum value in each data set because of the way placement of all data points on one curve is performed and is thus only approximate. The error statistics reported below were calculated without using the maximum value in each data set, and are transformed from fractional values from 0-1 to camera values from 0-255. The mean absolute value of the variation is 1.13, and the mean value is 0.58. The average of the noise when estimated from the calibration curve is 12.5. This value is close to the value of 13.6 obtained by directly estimating the dark noise (see section 2.6.1 below). The root mean square value of the variation is 1.45. The maximum error is 4.67 and occurs for a green sensor reading.

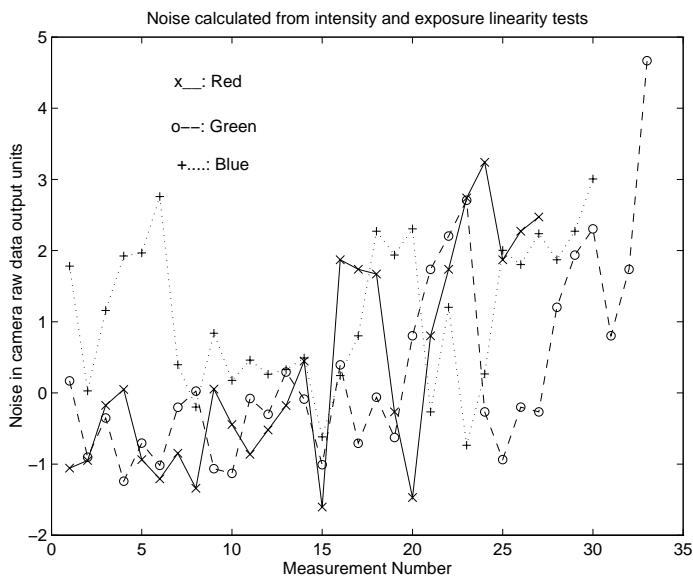


Figure 7: Variation from linearity - DCS-200

To quantify the slight variation of the scaled DCS-420 data points from the curve in Figure 6, we calculated the difference between the data point and the value on the curve corresponding to the scaled intensity, i.e. the difference between indirectly measured values of $\mathcal{F}^{-1}(r) - n$ and values obtained from the calibration curve. As for the DCS-200, this calculation assigns zero difference to the maximum value in each data set and is thus only approximate. The error statistics reported below were calculated without using the maximum value in each data set, and without scaling the linearized output to the camera output scale of 0-255.

The average absolute value of the variation was 0.0015. The root mean square value of the variation was 0.0021, approximately 0.5 units per 256 (for comparison with the variation for the DCS-200) and the maximum value was 0.0072, approximately 1.8 units per 256. As can be seen from the plots of Figure 8, the blue has most variation, and the red and green variations are comparable.

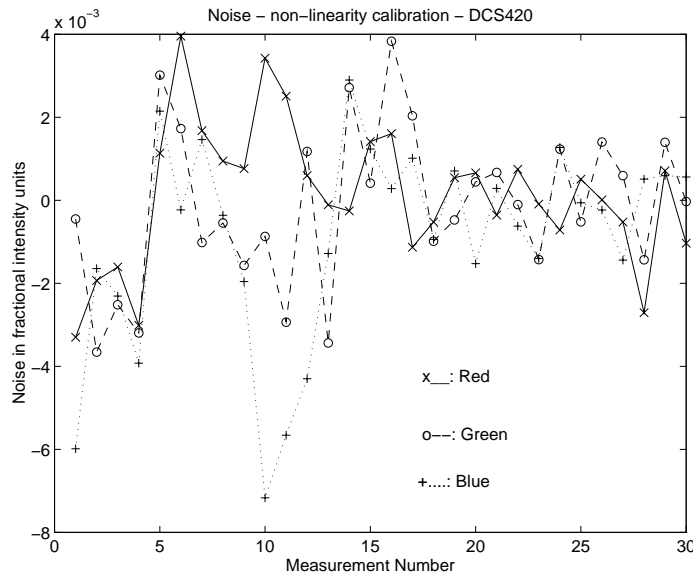


Figure 8: Variation from calibrated curve - DCS-420

2.6 Noise Measurements

We took a number of dark images at different times during our day-long experiments, and at different exposure durations. We first discuss the effect of exposure duration on dark current noise, and then the effect of aging.

2.6.1 Dark current noise as a function of exposure

Kodak DCS-200

The dark noise was averaged over the same rectangular area of the center field as the linearity measurements. The data are tabulated in Table 2. Dark noise shows some variation with exposure duration, up to 4 units, but is quite constant over the different color bands. The mean of the data tabulated is 13.61, 13.63 and 13.61 for red, green, and blue sensors respectively. The overall mean is 13.62. The variances for the three sensor types are 0.78, 0.79 and 0.81 respectively; the corresponding standard deviations are 0.88, 0.89 and 0.90. The overall variance about 13.62 is 0.79 with a standard deviation of 0.89. Variation is greatest for blue sensors and least for red, but the differences are slight.

The mean values may be compared to those obtained from the variation from linearity calculations in section 2.5. The value of 12.5 obtained there is close to the measured values. The variation values may be compared to the values obtained in section 2.5. The variation from linearity includes the dark noise variation, but is larger because it is not limited to the dark noise variation. It includes other non-linear aspects of the sensor response, including other noise sources like shot noise.

Figure 9 illustrates the fact that the variation of dark noise with exposure duration is not monotonic at low exposure durations. This could be because of inaccuracy in the mechanics of the shutter movement. At exposure durations of one-fourth of a second and higher the variation of dark noise with exposure duration is monotonically decreasing. This could be because the effects of dark current are averaged out at higher exposure durations.

Exposure time in seconds	Average Dark Noise Value in Camera Output Units		
	Red	Green	Blue
8	12.52	12.58	12.51
4	12.85	12.83	12.84
2	12.92	12.93	12.94
1	13.54	13.56	13.51
0.5	13.90	13.92	13.83
0.25	14.27	14.32	14.32
0.125	14.44	14.47	14.45
1/15	14.31	14.32	14.33
1/30	14.54	14.54	14.54
1/60	14.54	14.56	14.60
1/125	11.90	11.88	11.87

Table 2: Dark Noise vs. Exposure Duration, DCS 200.

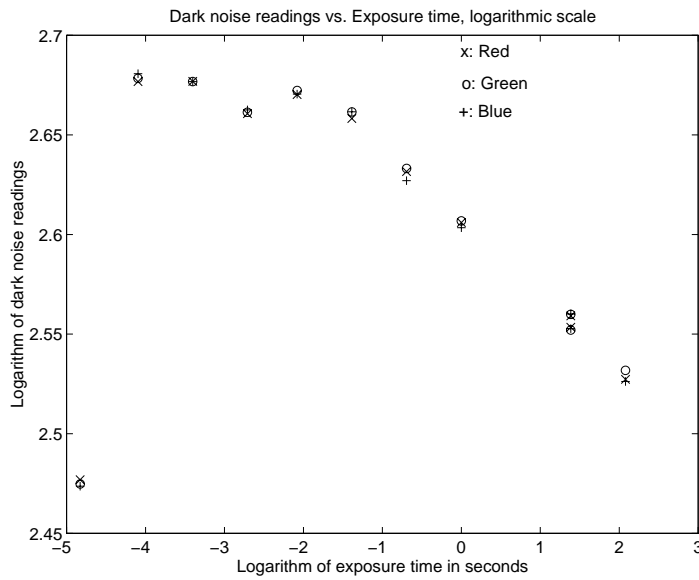


Figure 9: Dark noise vs. exposure duration - DCS-200

Kodak DCS-420

The average value of dark current noise is usually subtracted from readings that are known to be linear, i.e. readings predicted by equation (1). As the DCS-420 sensor outputs are the result of a non-linear function operating on the CCD measurements, (equation 2), the dark noise average cannot simply be subtracted from the sensor readings. In fact, our calibration curve (Figure 6) provides an indirect estimate of $\mathcal{F}^{-1}(r) - n$ and the variability from this curve provides an estimate of the effective additive noise. None-the-less, obtaining a direct measure of the dark noise variability seems useful for an estimate of acceptable errors in RGB prediction for camera calibration [7] (see section 3).

We took a few dark images (with the lens cap on) at various stages of the experiment, and at various exposure times. We calculated the average value over the same rectangle in the center field used for other measurements. The average value did not vary much. Its average over the different images was 25.02, 25.01 and 25.06 over red, green and blue sensors respectively. Its overall mean was 25.03. Individual variances about individual means were 0.2375, 0.2207 and 0.2203 for red, green and blue respectively. Its overall variance with respect to the overall mean was 0.2266, and the standard deviation 0.4760.

If we convert the dark noise standard deviation to the linear domain (using the average slope of the calibration curve) we get a value of 0.0019. This is a little lower than the measured deviations of the data from the curve. As with the DCS-200, the difference is explained by the fact that variation from the calibration curve includes the effects of other types of noise besides dark noise.

2.6.2 Dark current noise as a function of aging

The data of Table 2 were taken at the end of a day of experiments on the DCS-200, after 120 images were taken with the camera. The next morning, after just a few pictures, a few more dark noise images were taken. The average values of the dark noise images taken over the same rectangular area in the center-field of the camera are listed in Table 3.

The readings for 0.125 seconds are very close to but slightly below those taken earlier. The readings for 1/125 seconds, however, are above those taken earlier by more than 1 unit, an amount which is slightly higher than the standard deviation of the earlier set of readings. Even if this effect is real, it is small, and we suspect that treating the camera as a stationary device is satisfactory for most purposes.

Table 3: Dark Noise vs. Exposure Duration, DCS 200, Later Readings.

Exposure time in seconds	Average Dark Noise Value in Camera Output Units		
	Red	Green	Blue
0.125	14.05	14.04	14.02
1/125	13.08	13.15	13.08

3 Camera calibration

In this section, we describe the spectral calibration of the Kodak DCS-200 and Kodak DCS-420 digital cameras. The calibration procedure is based on the response models we developed and tested for these cameras in the previous section [6]. In this section we first describe how we collected the spectral calibration data. Then we describe simple methods for estimating the camera sensor spectral response functions. Finally, we determine if our estimates of the DCS-200 and DCS-420 can predict the camera responses for images of the Macbeth ColorChecker Chart (MCC).

3.1 Methods

For both cameras, we used the 8-bit acquisition software provided by Kodak. In this mode, the response of the DCS-200 is linear with intensity while the response of the DCS-420 is non-linear [6] (see section 2). The camera apertures were kept fixed through all the experiments reported here, at f4 for the DCS-420 and f5.6 for the

DCS-200. These are the same aperture settings we used to determine the camera response models.

To calibrate the camera spectral sensitivities, we measured camera responses to narrow band illumination. We created narrow band stimuli using light from a tungsten source passed through a monochromator (Bausch and Lomb, 1350 grooves/mm) and imaged onto a non-selective reflectance standard (PhotoResearch RS-2). We measured the integrated radiance of each narrow band stimulus using a spectroradiometer (PhotoResearch PR-650). The camera and the radiometer were placed at similar geometric positions with respect to the reflectance standard.

It is difficult to measure the exact spectral power distributions of narrow band sources using the PR-650, since the instrument itself has a bandwidth of 8nm, comparable to that of the narrow band lights. When we performed calculations that required an estimate of the spectral power distributions, we modeled them as narrow gaussians scaled so that they had the same integrated radiance as our measurements.

We extracted red, green, and blue (R, G, and B) sensor responses from the camera images and averaged these over a rectangular section in the center of the image (64×64 pixels for the DCS-420 and 30×25 pixels for the DCS-200). For the DCS-200, we excluded measurements outside of the camera’s linear operating range. We corrected the measured responses for the camera dark current by subtracting our estimate of its mean values. For the DCS-420, we used Table 1 to obtain linearized response values. To extend the quantization precision of the cameras, we varied the exposure duration across measurements. We normalized response data across exposure setting by dividing the measured linear response by the exposure duration.

3.2 Simple estimate

To perform calculations, we write a version of equation (2) that describes the entire calibration data set. Let \mathbf{r} , \mathbf{g} , and \mathbf{b} be vectors representing the R, G, B readings to a series of narrowband lights. The vectors \mathbf{r} , \mathbf{g} , and \mathbf{b} have K_r , K_g and K_b entries respectively, one for each of the narrowband stimuli used to calibrate the

corresponding sensor. Let the full spectrum of the i^{th} narrowband light be $s_i(\lambda)$, and let the unknown camera spectral sensitivities be $c_r(\lambda)$, $c_g(\lambda)$ and $c_b(\lambda)$. From equation (2) we have,

$$\mathbf{r} = \mathcal{F} \left(\begin{bmatrix} e(1) \sum_j c_r(\lambda_l + j\Delta\lambda) s_1(\lambda_l + j\Delta\lambda) \Delta\lambda \\ \vdots \\ e(i) \sum_j c_r(\lambda_l + j\Delta\lambda) s_i(\lambda_l + j\Delta\lambda) \Delta\lambda \\ \vdots \\ e(K_r) \sum_j c_r(\lambda_l + j\Delta\lambda) s_{K_r}(\lambda_l + j\Delta\lambda) \Delta\lambda \end{bmatrix} + \mathbf{n} \right) \quad (3)$$

where \mathbf{n} is a vector representing measurement noise with variation about the average dark noise value, $\Delta\lambda$ is the wavelength sampling for the radiometric measurements, and $e(i)$ is the exposure setting for the i^{th} measurement. The function \mathcal{F} is applied pointwise to each component of the vector it acts on. It is the identity for the DCS-200 and the calibrated static non-linearity for the DCS-420. Equations similar to the one above can be written for the readings \mathbf{g} and \mathbf{b} . The equations for $c_r(\lambda)$, $c_g(\lambda)$ and $c_b(\lambda)$ may be solved in a number of different ways. In the rest of this section and the next we discuss some possibilities.

The illumination incident on the camera is narrow-band. Using the i^{th} measurement taken under illumination s_i centred around λ_i and ignoring the noise variability, we may estimate the sensor response function $c_r(\lambda_i)$ as

$$c_r(\lambda_i) = \frac{\mathcal{F}^{-1}(r_i) - \bar{n}}{e(i) \sum_j s_i(\lambda_i + j\Delta\lambda) \Delta\lambda} \quad (4)$$

where r_i is the i^{th} component of \mathbf{r} , the quantity $\sum_j s_i(\lambda_i + j\Delta\lambda) \Delta\lambda$ is the integrated radiance of the i^{th} narrowband stimulus and \bar{n} is the mean of the noise. For CCD cameras, this mean is typically non-zero.

Equation (4) is the ‘simple’ estimate [2]. The function \mathcal{F} is the identity for the DCS-200 and $\bar{n} = 13.6$ the average measured dark noise value from the experiments detailed in [6] and section 2.6.1. For the DCS-420, the quantity $\mathcal{F}^{-1}(\mathbf{r}_i) - \bar{n}$ may be obtained from the calibration curve provided in Figure 6.

Figures 10 and 11 show plots of the simple estimates obtained for the DCS-200 and for the DCS-420 respectively. The plotted estimates are interpolated from the raw estimates obtained at wavelengths $\{\lambda_i\}$ to a 5 nm wavelength spacing in the range

380 nm to 780 nm. In the interpolation procedure, values for wavelengths outside the range where we had data were set to zero. Space limitations prevent us from tabulating the numerical values of the estimate in this report, but they may be found in [7]. The expression

$$\mathcal{F}(e(i) \sum c_r(\lambda_j) s_i(\lambda_j) \Delta \lambda_j + \bar{n}) \quad (5)$$

was used to calculate RGB values for sensors with the estimated spectral sensitivities. The function \mathcal{F} was taken to be the identity for the DCS-200. For the DCS-420, an inverse curve based on the calibration curve of Figure 6 was used. We compared the predicted RGB values to the measurements. Figures 12 and 13 show plots of the measured R, G and B values against the values indicated by expression (5) for the DCS-200 and the DCS-420 respectively. Tables 4 and 5 list the statistics of the estimation errors for the DCS-200 and the DCS-420 respectively.

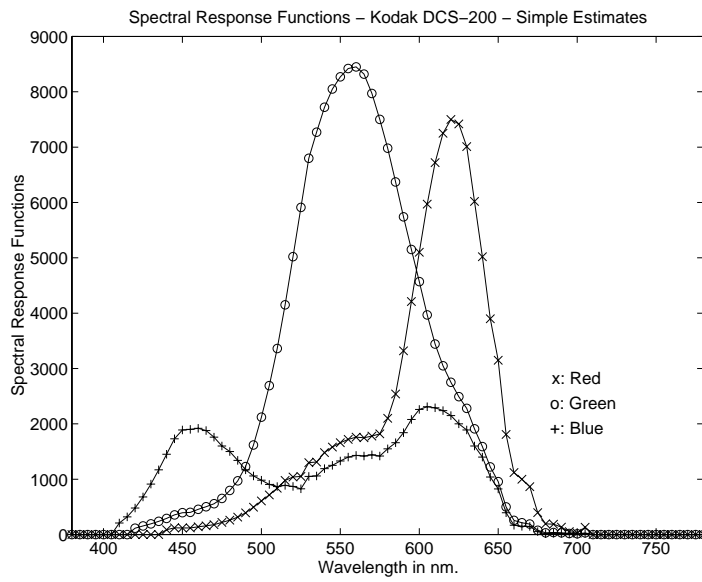


Figure 10: Spectral Response, DCS-200, Simple Estimate

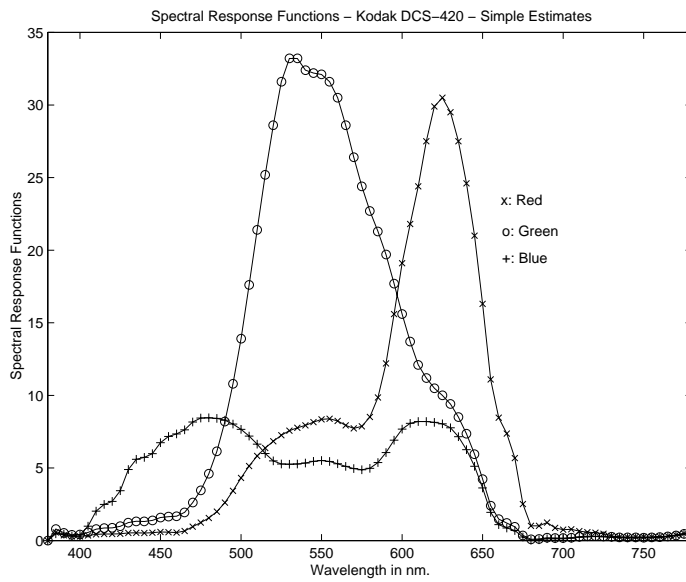


Figure 11: Spectral Response, DCS-420, Simple Estimate

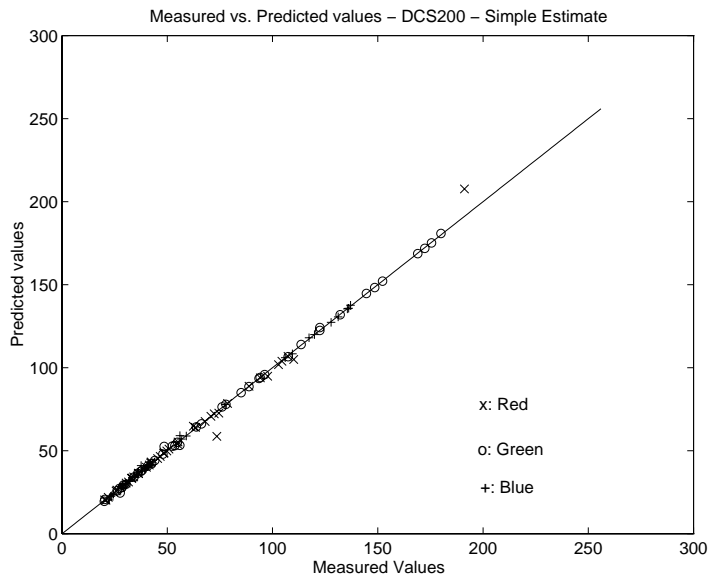


Figure 12: Measured vs. Predicted Values, DCS-200, Simple Estimate

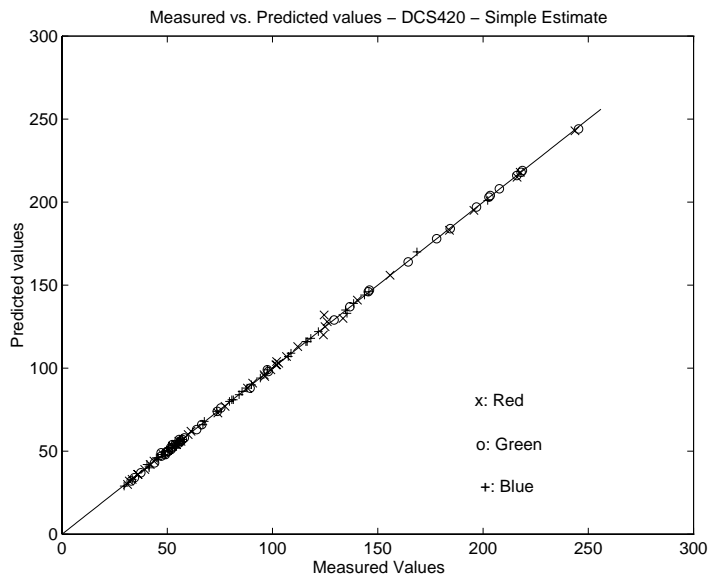


Figure 13: Measured vs. Predicted Values, DCS-420, Simple Estimate

Table 4: Statistics of Estimation Error - DCS-200 - Simple Estimate. RMS value of variation from linearity of DCS-200 is 1.45 [6].

Sensor Type	Mean of Absolute Error	Mean of Absolute % Error	RMS Error	Camera Noise Std. Deviation	Maximum Absolute Error	Maximum Absolute % Error
Red	1.34	1.60	3.68	0.88	16.46	20.27
Green	0.53	1.10	0.99	0.89	4.09	1.09
Blue	0.50	1.29	0.89	0.90	3.48	9.50

Table 5: Statistics of Estimation Error - DCS-420 - Simple Estimate. RMS value of variation from modelling curve of DCS-420 is 0.50 [6].

Sensor Type	Mean of Absolute Error	Mean of Absolute % Error	RMS Error	Camera Noise Std. Deviation	Maximum Absolute Error	Maximum Absolute % Error
Red	0.83	0.88	1.59	0.49	7.47	6.00
Green	0.57	0.88	0.74	0.47	1.96	4.17
Blue	0.59	0.91	0.78	0.47	2.36	3.99

3.3 Wiener and other estimation methods

The Wiener estimate for the spectral sensitivities may be calculated without the assumption that the illuminant sources used to obtain measurements were narrowband. We used a variant of the Wiener estimate that is guaranteed to produce all positive estimates.

The Wiener procedure requires that we regard the quantity to be estimated (say \mathbf{x}) as a gaussian random variable with known mean and covariance. We took the mean $\bar{\mathbf{x}}$ to be the simple estimate obtained in the previous section and constructed the covariance matrix $\kappa_{\mathbf{x}}$ by assuming that \mathbf{x} was the result of a first-order discrete Gauss-Markov process whose variance was equal to the variance of the entries of $\bar{\mathbf{x}}$ and whose entry-to-entry correlation was equal to the correlation between neighboring entries of $\bar{\mathbf{x}}$. We assumed that the entries of \mathbf{n} were independently and identically distributed with mean zero and variance equal to 2% of the maximum linearized sensor response (after correction for non-linearity, mean noise level, and exposure duration). We did this for each sensor and obtained results slightly better than those obtained in the previous section. Graphs of the Wiener estimates for the DCS-200 and the DCS-420 are presented in Figures 14 and 15. The spectral response estimates are interpolated as were the simple estimates. Space limitations prevent us from providing the numerical values of the spectral response estimates in this paper, but these values may be found in [7]. Scatter plots of measured values vs. values calculated from the Wiener spectral sensitivity estimates for the DCS-200 and the DCS-420 are plotted in Figures 16 and 17. Tables 6 and 7 list the statistics of the estimation errors for the DCS-200 and the DCS-420 respectively.

In contrast to our previous attempts to estimate the spectral sensitivities of the Kodak digital camera [2], the error for both the simple and Wiener estimates are low and close to the rms value predicted by the noise statistics for both cameras. Presumably one factor driving the small error is that we used many narrowband lights to calibrate the sensors. Also, since we used narrowband lights, the simple and the Wiener estimates are very similar. This would not have been so if we had used broadband lights [2], because the simple estimate assumes narrowband lights and is only accurate when this assumption is valid.

Non-linear estimation methods like Projections Onto Convex Sets (POCS) [5] are used when the Wiener estimation method gives results that clearly do not satisfy prior knowledge of the solution. For example, POCS would be used if the Wiener estimates gave unreasonable errors in the RGB values. Our estimates satisfy the three known constraints: the set of measured and predicted RGB values agree leaving room for reasonable noise; the filters are reasonably smooth; the filter transmissivities are non-negative. Hence, we did not attempt more complicated non-linear (particularly constrained) estimation methods.

3.4 Verification of estimates

For the DCS-200, we tested the spectral sensitivity estimates by collecting two images of the MCC under a tungsten illuminant. We compared the actual R, G, and B responses for the 24 color checker patches with values predicted from the spectral sensitivities of the camera and direct radiometric measurements of the light reaching the camera from each patch. To calculate the actual R, G, and B responses we averaged a roughly 20×20 pixel region at the center of each patch. The radiometric measurements were taken with the PhotoResearch PR-650 placed at approximately the same position as the camera. Figures 18 and 19 show the predicted vs. measured values for the simple and Wiener estimates respectively. Tables 8 and 9 list the error statistics. It is clear that the estimates are excellent, and perform well on data sets that were not used for the calibration.

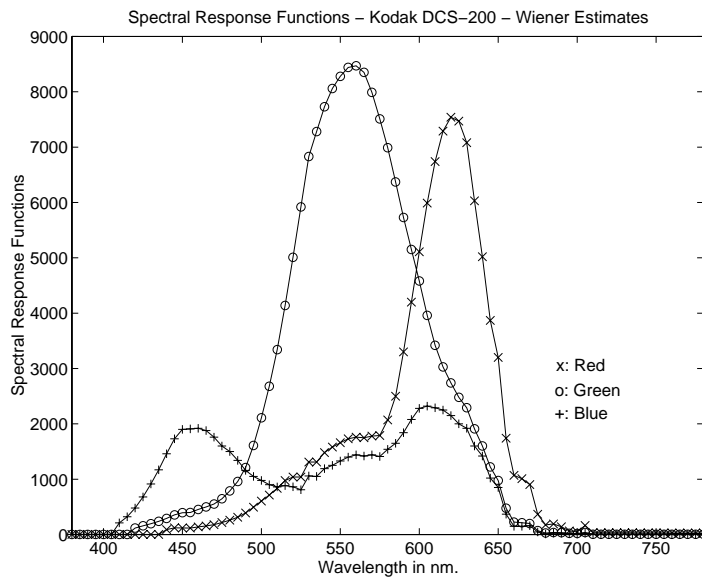


Figure 14: Spectral Response, DCS-200, Wiener Estimate

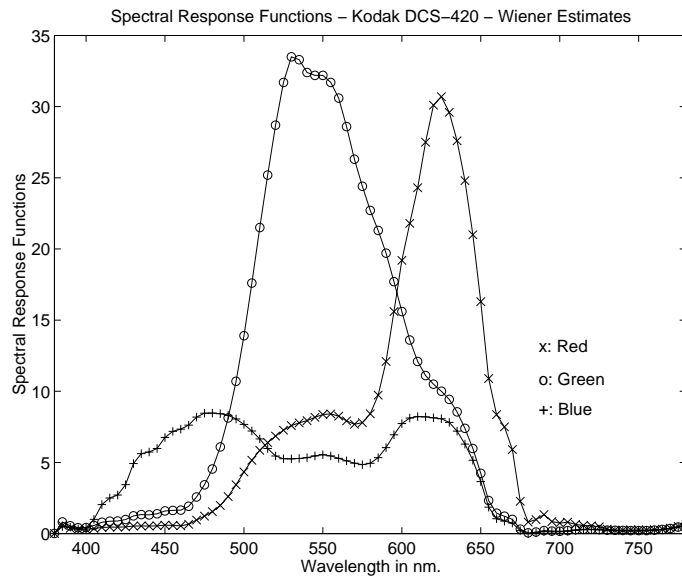


Figure 15: Spectral Response, DCS-420, Wiener Estimate

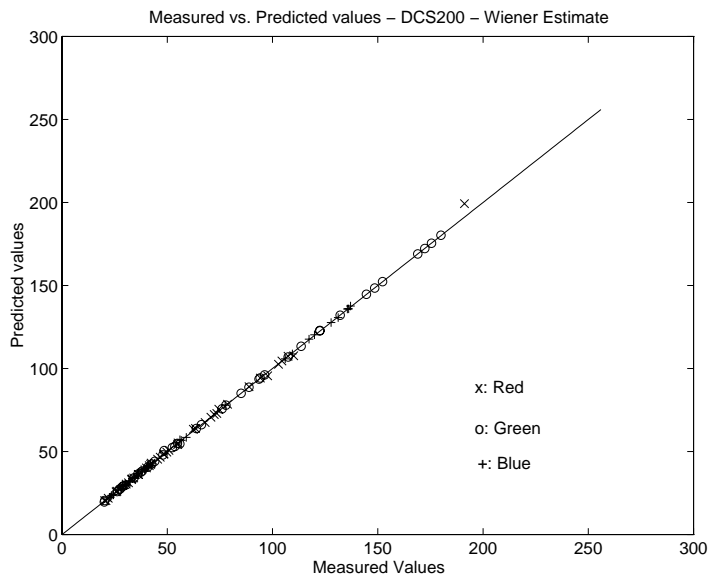


Figure 16: Measured vs. Predicted Values, DCS-200, Wiener Estimate

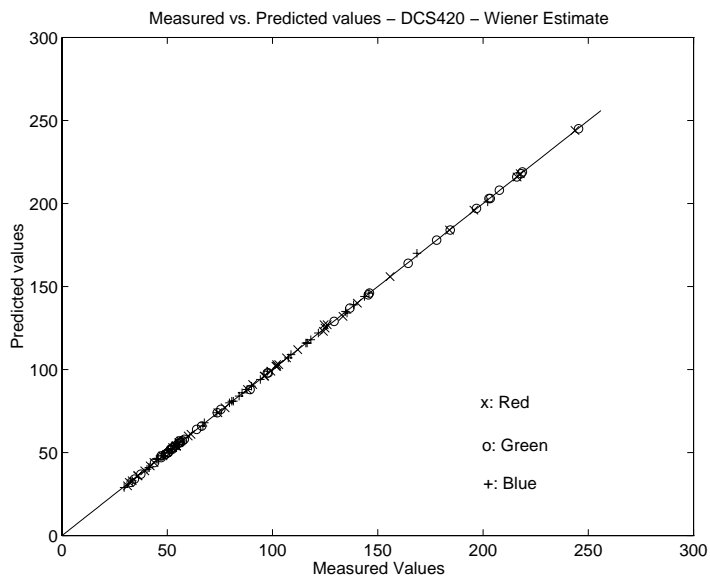


Figure 17: Measured vs. Predicted Values, DCS-420, Wiener Estimate

Table 6: Statistics of Estimation Error - DCS-200 - Wiener Estimates. RMS value of variation from linearity of DCS-200 is 1.45 [6].

Sensor Type	Mean of Absolute Error	Mean of Absolute % Error	RMS Error	Camera Noise Std. Deviation	Maximum Absolute Error	Maximum Absolute % Error
Red	0.53	0.65	1.42	0.88	8.07	4.22
Green	0.57	0.55	0.46	0.89	1.34	2.65
Blue	0.28	0.62	0.41	0.90	1.58	4.20

Table 7: Statistics of Estimation Error - DCS-420 - Wiener Estimates. RMS value of variation from modelling curve of DCS-420 is 0.50 [6].

Sensor Type	Mean of Absolute Error	Mean of Absolute % Error	RMS Error	Camera Noise Std. Deviation	Maximum Absolute Error	Maximum Absolute % Error
Red	0.40	0.51	0.62	0.49	2.47	3.69
Green	0.35	0.55	0.46	0.47	1.34	2.65
Blue	0.47	0.66	0.59	0.47	1.50	2.63

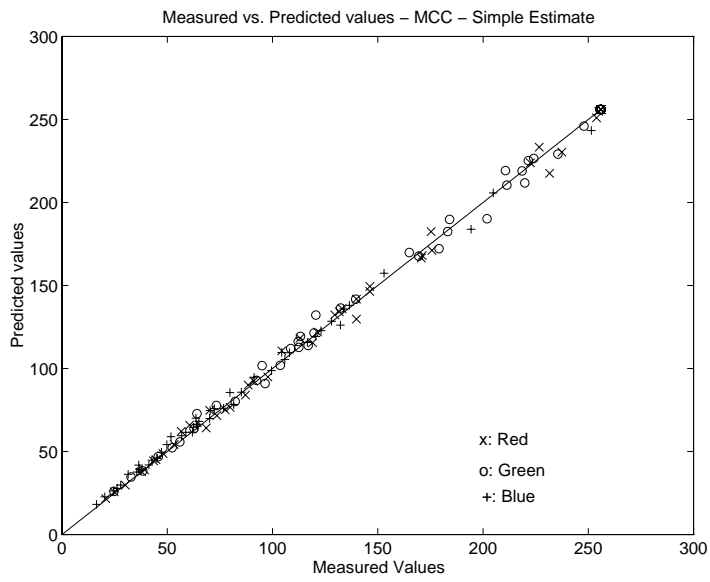


Figure 18: Measured vs. Predicted Values for MCC, DCS-200, Simple Estimate

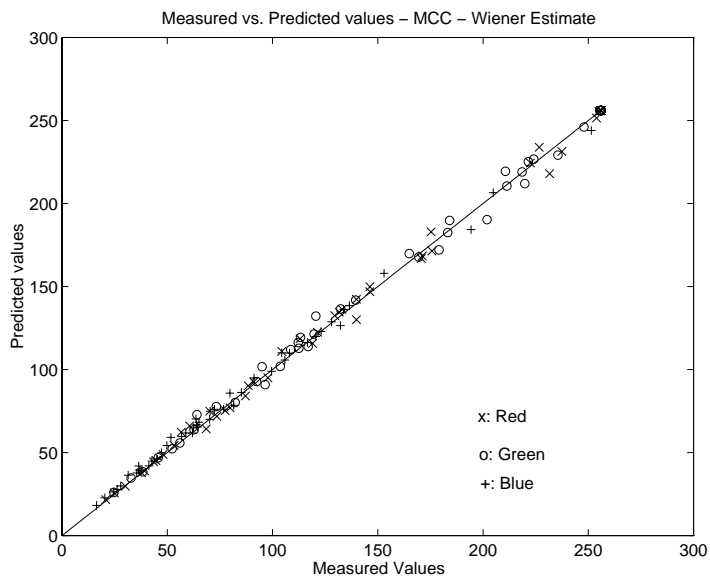


Figure 19: Measured vs. Predicted Values for MCC, DCS-200, Wiener Estimate

Table 8: Statistics of Estimation Error for MCC - DCS-200 - Simple Estimates. RMS value of variation from linearity of DCS-200 is 1.45 [6].

Sensor Type	Mean of Absolute Error	Mean of Absolute % Error	RMS Error	RMS of Variation in Patch	Camera Noise Std. Deviation	Maximum Absolute Error	Maximum Absolute % Error
Red	2.76	2.58	3.99	2.08	0.88	14.12	9.72
Green	2.84	2.40	4.25	1.96	0.89	11.78	13.59
Blue	2.74	4.55	3.56	1.83	0.90	10.44	15.53

Table 9: Statistics of Estimation Error for MCC - DCS-200 - Wiener Estimates. RMS value of variation from linearity of DCS-200 is 1.45 [6]

Sensor Type	Mean of Absolute Error	Mean of Absolute % Error	RMS Error	RMS of Variation in Patch	Camera Noise Std. Deviation	Maximum Absolute Error	Maximum Absolute % Error
Red	2.80	2.63	3.97	2.08	0.88	13.63	9.97
Green	2.85	2.41	4.27	1.96	0.89	11.70	13.63
Blue	2.81	4.68	3.60	1.83	0.90	9.95	15.80

4 Camera Simulator

In sections 2 and 3 we have shown that a linear model with the application of a static non-linearity (if necessary) is exceptionally good at predicting sensor response from digital image sensors. In this section, we describe the use of the linear model to simulate the response of a specific digital camera to a specified scene. The digital camera is defined by the values of a set of camera design parameters, and the scene is defined by intensity values as a function of space and wavelength. We also present experimental results that verify the accuracy of the simulator.

4.1 Simulator Description

The input to the simulator consists of a set of images which together represent an approximation of the intensity incident on the camera lens as a function of space and wavelength. At present, the input is a set of 31 images taken with the hyperspectral camera system [1]. The 31 images each represent a spatial distribution of the incident intensity over a narrow range of wavelength values. The simulator can also take a different representation of the input, for example a set of images each of which represents the spatial distribution of coefficients with respect to a basis set of principal components of a database of radiant spectra. In general, the simulator assumes that the intensity distribution as seen by the camera may be written as a weighted sum of a set of images, $(\mathbf{s}(m, n, k) = \sum_{i=1}^N c_i \times S_i(m, n) \times p_i(k))$ where $p_i(k)$ represent basis functions for the scene description with respect to wavelength. The simulator uses equation (1) to compute the simulated output image.

The parameters of the simulator are: (a) the sensor spectral sensitivities as a function of wavelength, sampled at the same rate as the representation of the input (or represented in terms of the same basis vectors as the input); (b) the exposure time; (c) the noise statistics (mean and variance); (d) the mosaic pattern; (e) the number of bits per pixel of the camera sensors.

A final step of the simulation, not described by equation (1), is to quantize the simulated output to the same number of bits as the simulated device. The output

raw data image of the simulator may be directly compared with the camera image for numerical verification. For visual quality judgements, we need to demosaic and color correct the outputs of the DCS-200 and the simulator and then compare the color images.

4.2 Simulator verification

This section describes the experiments performed to verify the accuracy of the simulator for color patches. The DCS-200 was used to take pictures of the MCC in a laboratory illuminated by an incandescent source (Kodak 4400 Slide Projector) at different exposure settings: 1/8, 1/15, 1/30, 1/60 and 1/125 seconds. The hyperspectral camera system was also used to acquire a 31-band hyperspectral image of the same chart under the same conditions. The hyperspectral image, the estimated DCS-200 spectral sensitivities, the exposure durations, the measured noise statistics and the bits per pixel value (8) of the DCS-200 were used to generate simulated images. The simulated images were compared both numerically and visually.

Figure 20 is a scatter plot of the real vs. simulated R, G, B values over all the shutter speeds studied in the experiment. It is clear that the agreement between real and simulated values is good. Table 10 lists the numerical error statistics of R, G, and B values averaged over the centre of each patch in both real and simulated images. Since the DCS-200 is an 8-bit camera, the numerical response values range between 0 and 255. The values in the table are computed from response values on this scale.

For purposes of comparison, the spatial variation in a dark noise image taken with the DCS-200 has a root mean square value of about 0.89 (see section 2.6.1). Linearity tests for this camera have shown that the root mean square value of the variation from linearity is 1.45 [6] (see section 2.5). Furthermore, the correspondence between predicted and empirical sensor values is consistent across exposure settings, supporting our assumption of linearity with respect to exposure duration - an assumption implicit in equation (1).

We visually compared the predicted and empirical sensor data after processing the

data with a simple demosaicing routine based on bilinear interpolation. (The complexity of the demosaicing routine is not expected to make a difference to visual quality, as the images consist of large color patches.) The real and simulated images have very similar appearances.

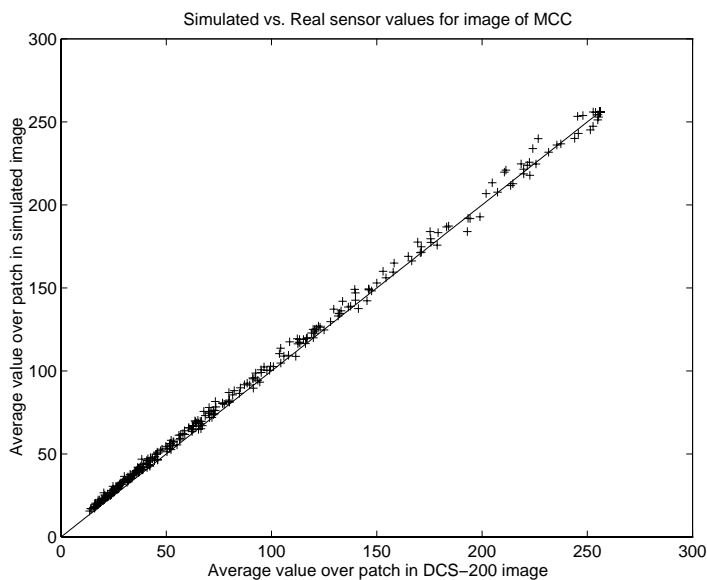


Figure 20: Scatter plot of MCC colour simulation

Table 10: Statistics of Simulation Error for MCC - DCS-200.

Exposure Setting in sec.	Mean of Absolute Error	Mean of Absolute % Error	RMS Error	Maximum Absolute Error	Maximum Absolute % Error
$\frac{1}{8}$	1.49	1.22	2.59	9.07	13.23
$\frac{1}{15}$	3.18	4.03	4.11	9.64	30.99
$\frac{1}{30}$	4.96	7.66	5.43	13.21	24.13
$\frac{1}{60}$	3.47	9.39	3.66	6.75	26.19
$\frac{1}{125}$	1.85	7.22	1.96	3.04	15.16

5 Conclusions and future directions

The use of a linear model with the application of a static non-linearity if necessary is appropriate for the calibration, modelling and simulation of the sensor responses of color filter array cameras. The color fidelity of output simulated using the linear model is good for a wide range of exposure settings. In the future we will incorporate a model for the optical system to simulate the effects of lens blur. The simulation of spatial effects (including the effect of a lens blur that may vary as a function of position with respect to center-field and wavelength, inter-sensor charge leakage and the mosaic pattern) on the visual quality of an image will be verified by using calibrated hyperspectral input images of scenes with richer spatial variation.

Acknowledgements: This work has been reported in preliminary form in [6, 7, 10, 11]. It was partly supported by a philanthropic grant from Hewlett-Packard to Prof. Brainard.

References

- [1] D. H. Brainard Hyperspectral Image Data, World Wide Web Site: <http://color.psych.ucsb.edu//hyperspectral/>, 1997.
- [2] P. M. Hubel, D. Sherman and J. E. Farrell, *A Comparison of Methods of Sensor Spectral Sensitivity Estimation*, Proc., IS&T/SID 2nd. Color Imaging Conference: Color Science, Systems and Applications, pp. 45:48, 1994.
- [3] T. S. Lomheim and L. S. Kalman, *Analytical Modeling and Digital Simulation of Scanning Charge-Coupled Device Imaging Systems* in Electro-Optical Displays ed. M. A. Karim, Marcel Dekker, 1992.
- [4] G. Sharma and H. J. Trussell, *Figures of merit for color scanners and cameras*, IEEE Trans. Image Proc., vol. 6, no. 7, pp. 990-1001, Jul. 1997.

- [5] H. J. Trussell and M. R. Civanlar, *The Feasible Solution in Signal Restoration*, IEEE Transactions on Acoustics, Speech, and Signal Processing, Vol ASSP-32, pp 201-212, 1984.
- [6] P. L. Vora, J. E. Farrell, J. D. Tietz and D. H. Brainard, *Digital color cameras - 1 - Response models*, Hewlett-Packard Company Technical Report, HPL-97-53, March 1997.
- [7] P. L. Vora, J. E. Farrell, J. D. Tietz and D. H. Brainard, *Digital color cameras - 2 - Spectral response*, Hewlett-Packard Company, Technical Report, HPL-97-54, March 1997.
- [8] *Programmer's Reference Manual Models: DCS200ci, DCS200mi, DCS200c, DCS200m*. Eastman Kodak Company, December 1992.
- [9] *MATLAB High-Performance Numeric Computation and Visualization Software, Reference Guide*, The MathWorks, Inc., 1992.
- [10] P. L. Vora, M. L. Harville, J. E. Farrell, J. D. Tietz, D. H. Brainard, 'Digital image capture: synthesis of sensor responses from multispectral images', Proceedings, SPIE and IS&T conference on Color Imaging: Device-Independent Color, Color Hard Copy, and Graphic Arts II, 10-14 Feb. 1997, San Jose, California, vol. 3018, pp. 2-11.
- [11] Poorvi L. Vora, Joyce E. Farrell, Jerome D. Tietz, David H. Brainard, "Linear models for digital cameras", Proceedings, IS&T's 50th Annual Conference, 18-23 May 1997, Cambridge, Massachusetts, pp. 377-382.